AGU PUBLICATIONS

JGR

Journal of Geophysical Research: Atmospheres

RESEARCH ARTICLE
10.1002/2015JD024452

Impact of urbanization patterns on the local climate of a tropical city, Singapore: An ensemble study

Xian-Xiang Li[1], Tieh-Yong Koh[2], Jagabandhu Panda[3], and Leslie K Norford[4]

[1]CENSAM, Singapore-MIT Alliance for Research and Technology, Singapore, [2]UniSIM College, SIM University, Singapore, [3]Department of Earth and Atmospheric Sciences, National Institute of Technology Rourkela, India, [4]Department of Architecture, Massachusetts Institute of Technology, Cambridge, Massachusetts, USA

Key Points:
- Urbanization patterns can impact UHI and rainfall
- Anthropogenic heat has strong influences on UHI and rainfall
- Urbanization modifies rainfall in two opposite ways

Correspondence to:
X.-X. Li,
lixx@smart.mit.edu

Citation:
Li, X.-X., T.-Y. Koh, J. Panda, and L. K. Norford (2016), Impact of urbanization patterns on the local climate of a tropical city, Singapore: An ensemble study, *J. Geophys. Res. Atmos.*, *121*, 4386–4403, doi:10.1002/2015JD024452.

Received 19 NOV 2015
Accepted 28 MAR 2016
Accepted article online 2 APR 2016
Published online 4 MAY 2016

Abstract The effect of urbanization and urbanization pattern on the thermal environment and local rainfall is investigated in the tropical coastal city, Singapore. The Weather Research and Forecasting (WRF) model is employed with 5 one-way nested domains and the highest horizontal resolution is 300 m. The urban effect is taken into account by a single-layer urban canopy model. Several scenarios with idealized urbanization patterns are designed and simulated for an ensemble of 28 members. In the asymmetric urbanization scenarios, in which either the southern or northern part of Singapore is urbanized while the other part is forest, the magnitude of urban heat island (UHI) intensity is higher than that in the symmetric urbanization scenario, in which the urban and forest land use is homogeneously distributed in Singapore. The anthropogenic heat (AH) associated with the urban areas will exacerbate the UHI intensity. Most of the rainfall in the examined cases occurs from late morning to afternoon when the sea breeze blows northeastward. The results suggest that sea breezes have stronger influence on the rainfall than the urbanization pattern since the downwind part always gets more rainfall than the upwind part. The urbanization and associated AH can have two opposite effects on the rainfall amount: increasing rainfall through increasing buoyancy by AH and decreasing rainfall through reducing evaporation by converting greenery to impervious surfaces. The ultimate effect is dependent on the relative strength of these two influences.

1. Introduction

As one of the extreme examples of human beings' changes to the natural environment, urbanization is continuously impacting our life in various aspects. Urbanization is not simply a microscale to local-scale effect, and it also demonstrates a regional-scale signature [*Y. Zhou et al.*, 2015]. A notable result of microclimatic changes caused by anthropogenic alterations to the Earth's surface is the urban heat island (UHI) effect [*Landsberg*, 1981], a phenomenon that the urban area is hotter than its surrounding rural area. Studies have shown that urban thermal conditions vary not only from those in rural surroundings but also within the urban area due to intraurban differences in land use and surface characteristics. The footprint of UHI effect can reach about 4 times of the urban size, with large spatiotemporal heterogeneities [*D. Zhou et al.*, 2015]. Urbanization also affects local winds and water cycles through the modification of natural surfaces and atmospheric conditions and further changes the local weather and climate system. While global-scale climate forcings are superimposed on the effects of the built environment on local transfers of heat and moisture, the impacts of cities on weather and climate may extend to regional and global scales by changing atmospheric composition, impacting components of the water cycle, and modifying the carbon cycle and ecosystems [*Shepherd*, 2005]. It has been shown that the global forcings and the forcings of the built environment are of similar order of impact, and some recent studies [*Georgescu et al.*, 2013, 2014] have explicitly made this important distinction between them. Therefore, a rising urgency exists to incorporate the scale-dependent built environment when local and strategical deployed measures (e. g., green roofs and cool roofs) are implemented to ameliorate the negative consequences on urban climate [*Georgescu et al.*, 2015].

There are various types of UHI [*Oke*, 1976], depending on the temperature used to define it. Here we focus on the urban canopy layer UHI, which measures the thermal environment below the average building height and with immediate impact on human comfort on a daily basis. One major effect of urbanization is the general reduction of the surface albedo, the ratio of outgoing shortwave radiation to that of incident shortwave

radiation in a three-dimensional environment. Lower albedo is due in part to darker surface materials making up the urban mosaic and also to the effects of trapping shortwave radiation by the vertical walls and the urban, canyon-like morphology [*Heisler and Brazel*, 2010]. The relative lack of vegetation in urban areas also contributes to the warmer environment than the surrounding rural areas. However, a recent report [*Zhao et al.*, 2014] argued that instead of the reduction in evaporative cooling in urban areas, it is the lower efficiency of convecting heat to the lower atmosphere (which depends on local background climate) in North American cities that contributes strongly to UHI. Anthropogenic heat (AH) is the energy released from human sources such as vehicles, commercial and residential buildings, industry, power plants, and human metabolism [*Quah and Roth*, 2012]. AH can greatly affect the urban environment by directly changing the surface air temperature and by indirectly modifying urban boundary layer structure, precipitation, and other conditions [e.g., *Ichinose et al.*, 1999; *Bornstein and Lin*, 2000; *Lin et al.*, 2008; *D. Li et al.*, 2013; *Bohnenstengel et al.*, 2014].

The influences of UHIs on human society include effects on human health and comfort, energy use, air pollution, and water use. The UHI during heat wave episodes (e.g., the 2003 summer heat wave in Europe) can pose a significant risk to human health or even life. Coastal, tropical, and rapidly growing cities are especially vulnerable to higher temperatures and impacts of urbanization [*Heisler and Brazel*, 2010]. In the long term, urbanization also has an irreversible impact on decadal surface temperature trends. For example, rapid urbanization in China during 1978–2001 has resulted in a surface temperature increase of 0.05 per decade [*Zhou et al.*, 2004]. More risks are expected as the sizes of urban areas grow continuously and the climate changes globally [*Hunt et al.*, 2013]. However, it must be pointed out that not all UHI effects are viewed as negative. In cold climates, UHI impacts may help reduce hazards of ice and snow in the city [*Voogt*, 2002], and winter comfort may be enhanced.

In addition to the UHI in downwind areas [*D.-L. Zhang et al.*, 2009, *Zhang et al.*, 2011], urbanization can also affect precipitation [*Bornstein and Lin*, 2000; *C.-L. Zhang et al.*, 2009; *Miao et al.*, 2011], an important component of the land-atmosphere interactions. Observations have shown warm seasonal rainfall increases of 9% to 17% over and downwind of major cities [*Changnon*, 1968; *Landsberg*, 1970; *Huff and Changnon*, 1972]. Possible mechanisms by which urbanization impacts precipitation or convective clouds have been identified as one or a combination of the following [*Shepherd*, 2005]: (1) enhanced convergence owing to increased surface roughness in the urban environment, (2) destabilization due to UHI thermal perturbation of the boundary layer and resulting downstream translation of the UHI circulation or UHI-generated convective clouds, (3) increased concentration of aerosols in the urban environment for cloud condensation nuclei, or (4) bifurcation or diversion of precipitating systems by the urban canopy or related processes. There are relatively limited studies of the impact of urbanization on precipitation compared with the extensive investigation of UHI. Some debate exists regarding the precipitation enhancement over and downwind of urban areas (see *Lowry* [1998], *Shepherd* [2005], and *Rosenfeld et al.* [2008] for more details). While the debate is continuing, more observational and numerical work is required to improve our understanding of this topic.

Extreme precipitation events (drought and flooding) in urban areas are the major hazard that motivates research work in urban-induced precipitation. Urban-enhanced precipitation events in conjunction with the increased extent of impervious surface have resulted in heavy runoff/urban flooding events [*Shepherd et al.*, 2011]. Therefore, the possible implications of urban-induced precipitation on the design of urban drainage systems should be taken into account [*Burian et al.*, 2004].

This study will investigate the impact of urban land use pattern on local climate in a tropical city, Singapore, with ensemble numerical simulations using the Weather Research and Forecasting (WRF) model. Unlike other cities with more development space, the city state of Singapore has limited area for further urbanization. Instead of looking at increasingly converting more nonurban land use to urban land use, Singapore must explore possible changes to the urbanization pattern (or, more broadly, land system architecture) [*Turner et al.*, 2013]. The objective of this research is to understand the effect of different urbanization patterns on local air temperature and precipitation.

2. Model Configuration and Experiment Design

2.1. The Study Area

Singapore is an island state located between 1°09′N to 1°29′N and 103°36′E to 104°25′E. Its climate is a typical wet equatorial type (Köppen classification: *Af*) [*Essenwanger*, 2001] with uniformly high monthly mean temperature (26–27.7°C) and annual rainfall (≈2300 mm). Singapore is located at the southern tip of the

Malay Peninsula and is affected by monsoons. The Northeast monsoon season from December to March, which is associated with the highest monthly rainfall and weaker winds, and the Southwest monsoon season from June to September, which corresponds to a relatively drier period, are separated by two brief intermonsoon or premonsoon periods [*Chia and Foong*, 1991]. There is no large and pronounced topography. The highest natural point is Bukit Timah at 164 m above sea level, which is exceeded in height by the tallest buildings in the central business district (CBD). This makes the study almost free of topographic effects, and our focus will be solely on the urbanization effect. There are ongoing land reclamation projects (mostly along the southern coastline), which have increased the land area to the current 704 km^2.

With a population reaching 5 million in 2011, Singapore has undergone dramatic urbanization during the past 45 years. The built-up area of Singapore has increased from 28% in 1955 to 50% in 1998, while the farm area and forest have decreased correspondingly [*Chow and Roth*, 2006]. Most of the urbanization is associated with the building of high-rise housing estates around the island, high-rise offices in the CBD in the south and industrial factories in the west.

2.2. The WRF Model

Numerical simulations in this study were performed with the WRF model [*Skamarock et al.*, 2008] version 3.2.1 with Advanced Research WRF dynamics core developed by the National Center for Atmospheric Research. The WRF model is a fully compressible, nonhydrostatic model with a terrain-following mass coordinate system and is designed to simulate or predict regional weather and climate. The WRF model is applied to the 5 one-way nested domains shown in Figure 1a. The horizontal resolutions (grid sizes) of these five domains are 24.3 km (76×76), 8.1 km (79×91), 2.7 km (112×112), 0.9 km (112×112), and 0.3 km (211×130). In the vertical direction, there are 38 full sigma levels from the surface to 50 hPa, with the lowest 14 levels resolving the planetary boundary layer (PBL).

Several physical parameterization schemes are employed in the WRF system to account for different physical processes. The Noah land surface model provides surface sensible and latent heat fluxes and surface skin temperature as lower boundary conditions to WRF. It can be coupled to various urban canopy models (UCM) through the urban fraction parameter (F_{urb}) that represents the proportion of impervious surfaces in the WRF subgrid scale. The UCM coupled to the WRF/Noah system in this study is the single-layer urban canopy model (SLUCM) developed by *Kusaka and Kimura* [2004]. This UCM has an intermediate level of complexity among the available UCMs for WRF. It assumes infinitely long street canyons parameterized to represent urban geometry but recognizes the three-dimensional nature of urban surfaces [*Chen et al.*, 2011]. More details of the UCM parameters used in this study can be found in *X.-X. Li et al.* [2013].

Other physical parameterizations employed in this study are: rapid radiative transfer model longwave radiation scheme, Dudhia shortwave radiation scheme, Mellor-Yamada-Janjić turbulence kinetic energy PBL scheme, Monin-Obukhov surface layer scheme, Goddard microphysics scheme, and Kain-Fritsch cumulus scheme (for d01 and d02 only).

It is noteworthy that with the fine horizontal resolution of the current study, the grid sizes fall within a "terra incognita" [*Wyngaard*, 2004] or grey zone in modeling the PBL. The smallest resolvable scale for such subkilometer resolutions is comparable to the scale of large eddies in the convective boundary layer. This makes the assumptions of traditional PBL parameters invalid. On the other hand, the subgrid-scale turbulence parameterizations of large-eddy simulation (LES) models require the smallest resolvable scale in the intertial subrange (usually less than 100 m). Hence, neither the traditional PBL schemes nor LES performs appropriately at this grey zone [*Shin and Dudhia*, 2016]. Therefore, the momentum and heat fluxes throughout the PBL may be partly resolved and partly parameterized. Several attempts have been made to tackle this issue by modifying traditional PBL schemes [e.g., *Honnert et al.*, 2011; *Boutle et al.*, 2014; *Ito et al.*, 2015; *Shin and Hong*, 2015] or using LES [e.g., *Zhou et al.*, 2014; *Efstathiou and Beare*, 2015]. Recently, more and more numerical studies at grey zone resolutions have been performed to study urban climate [e.g., *Miao et al.*, 2009; *Salamanca et al.*, 2012] and even tropical cyclone [*Green and Zhang*, 2015]. Apparently, more is needed for better understanding the turbulence parameterizations at subkilometer resolution. However, this is beyond the scope of the current study, and we leave it for future study.

2.3. Input Data

To represent the ever-growing urbanization of Singapore, up-to-date high-resolution land use/land cover data for Singapore have been obtained from Satellite Pour l'Observation de la Terre images and the Singapore

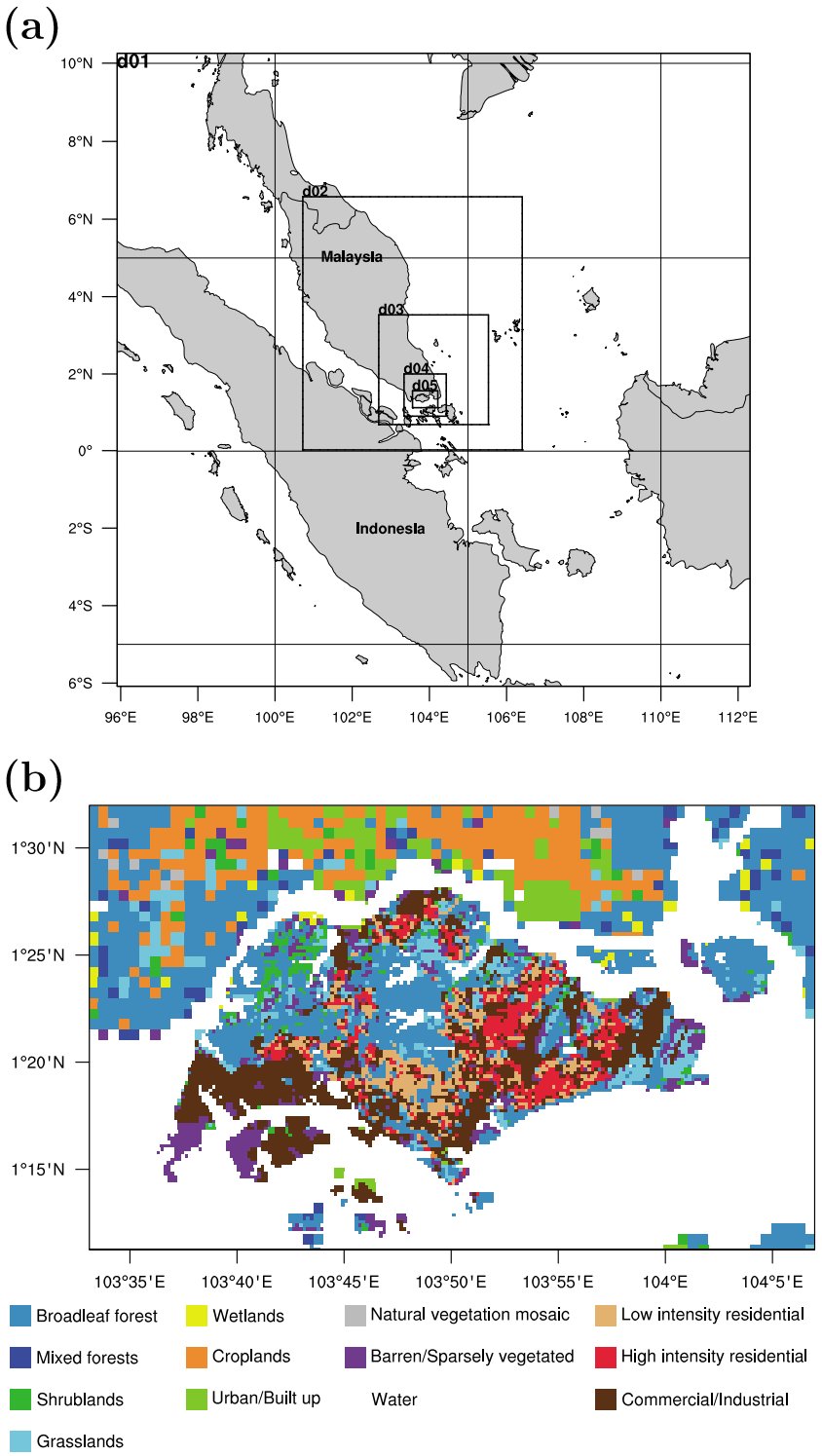

Figure 1. Configuration for WRF simulations. (a) The five nested domains; and (b) the land use/land cover map for domain d05 as used in the CONTROL experiment, which is centered on Singapore island.

Table 1. Summary of the Designed Experiments

Experiments	Land Use Pattern	Peak AH Value (W m^{-2})
SURB	South: urban; north: forest	39.0
NURB	South: forest; north: urban	97.5
NURBS	South: forest; north: urban	39.0
HURB	Homogeneous urban and forest	58.0
HURBS	Homogeneous urban and forest	39.0
FOREST	All Singapore is forest	0

Master Plan 2008 (Figure 1b). In accordance with the SLUCM's classification scheme, which restricts the urban land use/cover to three categories, the urban surface is further classified as high-intensity residential, low-intensity residential, and commercial/industrial areas. For regions outside Singapore, the Moderate Resolution Imaging Spectroradiometer 24-category land use/land cover data are used. The high-resolution topography data from Shuttle Radar Topography Mission [http://www2.jpl.nasa.gov/srtm/] are retrieved for the three inner domains. A diurnally varying AH profile from *Quah and Roth* [2012] is prescribed in the SLUCM.

The initial and boundary conditions are taken from the National Centers for Environmental Prediction 6-hourly operational Global Final Analyses data at a 1.0° × 1.0° resolution.

2.4. Ensemble Method

To study the urban environment under nonlinear dynamics and with the coexistence of many environmental variables, we adopt the ensemble approach, in which simulations are carried out for numerous cases with similar synoptic conditions and the ensemble statistics are obtained from these simulations. To select the members of the ensemble, the weather conditions in Singapore from 2007 to 2008 were classified into eight categories based on (1) CAPE (convective available potential energy): high (>1746 J kg^{-1}) or low (<364 J kg^{-1}), (2) advection (the wind speed at 850 mb): high (>7 m s^{-1}) or low (<3 m s^{-1}), and (3) monsoon season: intermonsoon or monsoon. These classification criteria are based on the statistics of the sounding record from the Changi meteorological station from 1990 to 2011. The criterion of high or low category is the 75th and 25th percentile of the wind speed and CAPE, respectively. In this study, the ensemble members are from the category of high CAPE, low advection, and intermonsoon (pre-Southwest monsoon) season. The intention for selecting this category is to minimize synoptic influences while maximizing the role of urban areas in the meteorological processes. A total of 28 members from April to May in 2007–2008 are selected to form the ensemble. All ensemble member case studies that were simulated with the WRF model are verified to belong to the high CAPE and low advection category. Each member has a 36 h simulation time starting at 12 UTC (= LT −8 h) of the previous day and ending at 00 UTC of the next day. The first 12 h are treated as spin-up time and neglected when calculating the ensemble statistics.

It must be pointed out that due to the selection of ensemble members during intermonsoon season in April and May, the results to be presented in the next section will be valid for this specific season in Singapore, especially the results for rainfall, which is more seasonally dependent and has significantly different dynamics (e. g., rainfall distribution and intensity) during monsoon and intermonsoon seasons [*Lim and Samah*, 2004]. In this study, the synoptic signals (e. g., monsoon) are precluded from affecting the urban-dominated processes in order to focus on the local effect induced by urbanization.

2.5. Experiment Design

In order to study the effect of the symmetric and asymmetric urban land use patterns in Singapore, a series of idealized experiments is designed, focusing on both the location of urban area and the associated AH. The current, realistic land use map of Singapore (as shown in Figure 1b) and AH (see *X.-X. Li et al.* [2013] for more details) are used in the CONTROL experiment (the same as the CONTROL experiment in *X.-X. Li et al.* [2013]). The details of other experiments can be found in Table 1 and will be elaborated below. To focus on the extreme scenario of urbanization and avoid the noise introduced by other factors, the urban area in these idealized experiments will be represented by commercial and industrial land use type only. This simplification will inevitably introduce some uncertainties compared to the case with realistic land use. However, it is assumed that these uncertainties will be eliminated by using the same urban land use type in all the idealized experiments. In addition, this simplification is in accordance with the ongoing urbanization all over Singapore by replacing low-rise, low-intensity buildings with high-rise, high-intensity buildings. The FOREST experiment,

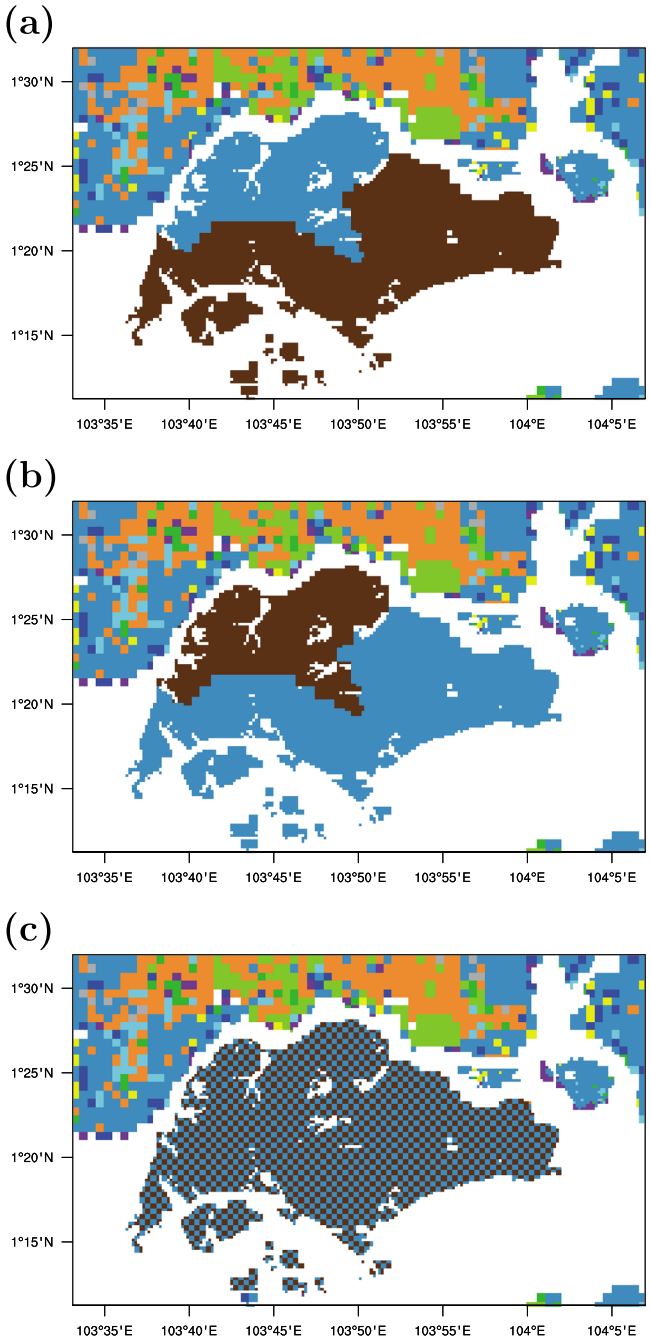

Figure 2. The land use/land cover map for domain d05 as used in the (a) SURB, (b) NURB/NURBS, and (c) HURB/HURBS experiments. The legend is the same as in Figure 1b.

in which all Singapore (except water bodies) is converted into evergreen broadleaf forest, is used as the rural reference for computing UHI intensity.

In the SURB experiment (Figure 2a), the southern part of Singapore is converted into urban area while the northern part is converted into forest area. This can be viewed as a simplification of the current urbanization pattern (as shown in the CONTROL experiment, Figure 1b). In the NURB experiment (Figure 2b), the northern part of Singapore is converted into urban area while the southern part becomes forest. The HURB experiment (Figure 2c) creates a homogeneous distribution of urban areas and forest by alternating these two land use types over grid boxes in Singapore. In these experiments, the HURB experiment represents a symmetric urbanization pattern, while SURB and NURB experiments are asymmetric urbanization patterns.

The same urban parameters used in the CONTROL experiment [*X.-X. Li et al.*, 2013, Table 1] are used for all other experiments, with the exception of the peak AH. The diurnal profile and peak value of AH used in the CONTROL experiment are documented in detail in *X.-X. Li et al.* [2013, Figure 3]. The same diurnal profile of AH is used in the above mentioned experiments. In order to remove the unrealistic excessive direct warming that would have occurred due to AH from converting all urban land use types to the commercial/industrial land use type, we have to roughly preserve the same domain-averaged 1 day integrated sensible heat flux as the CONTROL experiment in domain d05. Therefore, with some sensitivity tests of different peak AH, the peak AH values for the SURB, NURB, and HURB experiment are modified from 113 W m^{-2} in the CONTROL experiment to 39.0, 97.5, and 58.0 W m^{-2}, respectively. However, due to the important role played by AH in altering the urban environment (as demonstrated in *X.-X. Li et al.* [2013]), two more experiments using the same peak AH value and diurnal profile as in the SURB experiment, i.e., NURBS and HURBS, are added in order to compare more consistently the effect of AH.

3. Results and Discussions

In this section, the effect of urbanization patterns (as described in the previous section) on the local climate of Singapore will be examined based on the WRF-SLUCM simulation results. Unless otherwise specified, the numerical results presented in this section are for domain d05.

3.1. Urban Heat Island

The coupled WRF/UCM model's performance in reproducing the surface air temperature and surface energy balance has been evaluated by *X.-X. Li et al.* [2013]. The 2 m air temperature and specific humidity calculated from the coupled WRF/UCM model were validated against those from a sensor network operated across the Singapore island. A mean bias of −0.27°C for temperature was achieved, while a worse agreement of specific humility (about 10% underprediction) was reported. In addition, the surface energy balance components from the model were compared favorably with the observed values from a flux tower located within an urban neighborhood [*X.-X. Li et al.*, 2013]. In this section, the model will be used to investigate the UHI characteristics of Singapore under different urbanization scenarios.

3.1.1. Calculation Method of UHI Intensity

The canopy-layer UHI intensity due to urbanization can be calculated in two ways. The first way is the traditional difference in the 2 m air temperature, T_2, between urban and nearby undeveloped rural areas (evergreen broad leaf forest in this case). The second is the difference in the 2 m temperatures between the CONTROL and FOREST simulations, which is termed as "urban increment." This method largely removes impacts of clouds or topography that might alter the surface temperatures [*Bohnenstengel et al.*, 2011]. In this section, the second method is adopted in order to facilitate the comparison between different experiments. The calculated UHI intensity is further averaged over the same land use type (commercial/industrial) in domain d05.

The local circulations (sea/land breezes) can play a significant role in modulating UHI intensity in a coastal urban environment [*Joseph et al.*, 2008; *X.-X. Li et al.*, 2013] and will create an ambient temperature gradient in Singapore. To standardize the geographical sampling and thus minimize the impact of local circulations when comparing UHI intensity in different experiments, the UHI intensities of the HURB/HURBS experiments are split into two parts, i.e., southern and northern part (hereafter denoted as HURB/HURBS-south and HURB/HURBS-north, respectively) in accordance with the SURB and NURB experiments.

3.1.2. Effect of Urbanization Patterns

The symmetric and asymmetric urbanization patterns in Singapore can affect the distribution of UHI intensity. With the contiguous urban areas in the asymmetric urbanization experiments (SURB and NURBS, Figure 3), the urban canopy will not only increase the total amount of AH release but also make the released heat not easily removed by horizontal advection as neighboring areas are as warm. As a result, the magnitudes of the UHI intensity in the asymmetric urbanization settings are consistently higher than the corresponding part of the symmetric urbanization experiment, HURBS (Figures 3a and 3c). A further check by utilizing a paired, unequaled *t* test reveals that the above observation is statistically significant during early morning (2:00 to 7:00 LT) with p value < 0.01, but not significant during daytime. A notable phenomenon in Figures 3a and 3b is that the UHI discrepancy between asymmetric/symmetric urbanization experiments is larger during nighttime (late evening to early morning) than during daytime. To elaborate this, it is necessary to introduce here surface energy balance, which is the key to understanding the surface air temperature evolution. The surface energy balance for urban area reads

$$Q^* + Q_F = Q_H + Q_E + \Delta Q_S, \quad (1)$$

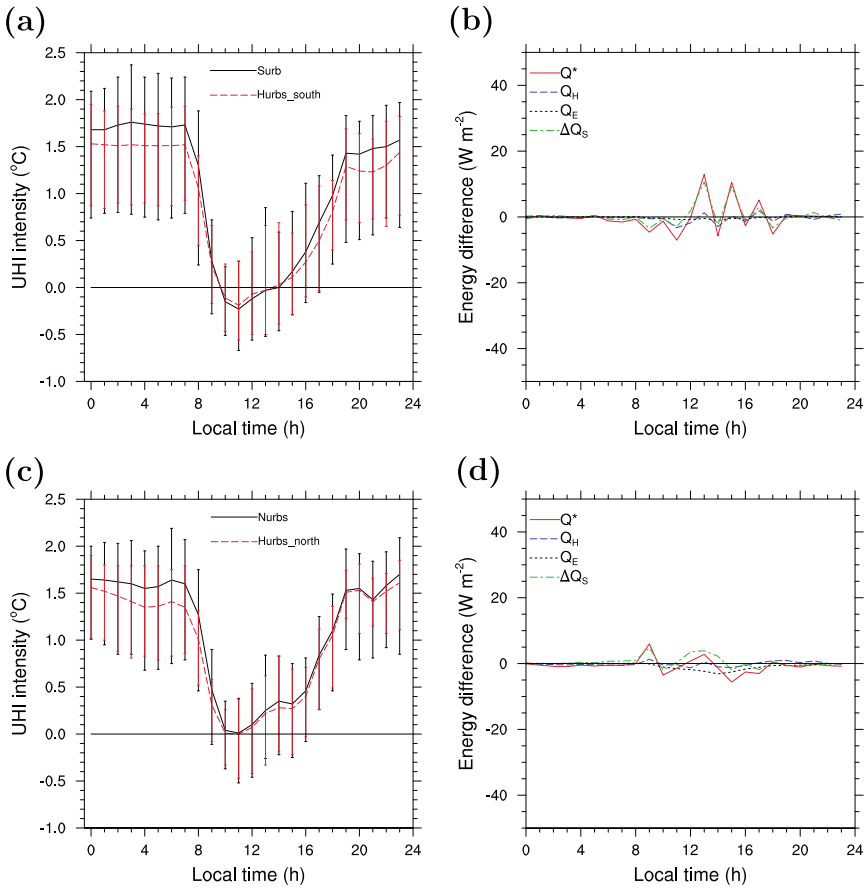

Figure 3. UHI intensity and energy balance change comparison between asymmetric and symmetric urbanization patterns. (a) UHI intensity of SURB and HURBS_south; (b) difference of energy change between SURB and HURBS-south relative to FOREST; (c) UHI intensity of NURBS and HURBS_north; and (d) difference of energy change between NURBS and HURBS_north relative to FOREST. The vertical bars indicate the maximum and minimum UHI intensities.

where Q^* is the net all-wave radiation, Q_H and Q_E are the turbulent sensible and latent heat flux, respectively, ΔQ_S is the net heat storage, and Q_F is the anthropogenic heat flux. The net heat storage includes the energy storage within the buildings, the road and underlying soil, and for some models the air space within the street canyon [*Grimmond and Oke*, 1999]. Here the net heat advection is assumed to be negligible. During daytime, net solar radiation Q^* dominates the surface energy balance, while during nighttime, the Q_F becomes the dominant factor [*X.-X. Li et al.*, 2013]. The differences in the energy balance change (averaged over all urban grid cells) between asymmetric and symmetric experiments relative to the FOREST experiment are shown in Figures 3b and 3d. No significant differences of Q_H can be observed during daytime or nighttime. In WRF, however, the 2 m air temperature T_2 is only a diagnostic variable and can be calculated as

$$T_2 = T_s - \frac{Q_H}{\rho c_p C_{h2} U_2}, \tag{2}$$

where T_s is the surface skin temperature, ρ is the air density, c_p is the specific heat capacity of air, C_{h2} is the transfer coefficient at 2 m, and U_2 is the wind speed at 2 m [*Li and Bou-Zeid*, 2014]. Therefore, T_2 is primarily determined by T_s when Q_H and U_2 are almost the same across each experiment. The T_s for each experiment (averaged over all the urban grid cells) is depicted in Figure 4, and obviously, T_s in SURB and NURBS is higher than in the HURBS-south and HURBS-north, respectively, during the early morning but does not differ much in daytime. The reason for this can be attributed to the AH; in SURB and NURBS, the total AH is much higher than in HURBS-south and HURBS-north, respectively, due to their different urban ratios. The effect of AH will be further examined in a later section.

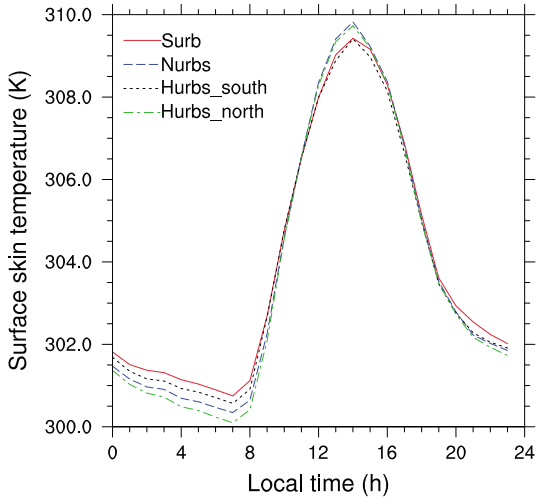

Figure 4. The averaged surface skin temperatures T_s in SURB, NURBS, and HURBS_south and HURBS_north, which are calculated over all the urban grid cells in the respective experiments.

It is noteworthy that in Figure 3a there are some negative UHI values during noon, which is referred to as the urban cool island effect [*X.-X. Li et al.*, 2013]. This urban cool island results from different heat capacities in urban and rural areas, as well as the shading effect in urban areas, especially for commercial/industrial areas where buildings are high.

3.1.3. Effect of Local Circulations

As a coastal city located at the southern tip of the Malay Peninsula, Singapore has complex local circulations (sea and land breezes) driven by differential heating between the land and sea. These local circulations are important mechanisms for air pollution transport in coastal regions, as well as for the occurrence of local rainfall. The sea breeze usually develops when solar irradiation is maximum, i.e., around 13:00 LT, with a strength of 4 m s^{-1}. During the late night/early morning, a much weaker land breeze (< 1 m s^{-1}) blows from the Malay Peninsula to the sea [*X.-X. Li et al.*, 2013]. These sea/land breezes are only part of the sea/land breeze systems commonly found in the Malay Peninsula. Due to the complex coastlines and relatively flat terrain in the southern Malay Peninsula, there are often complicated interactions between sea breezes in this area [*Joseph et al.*, 2008; *X.-X. Li et al.*, 2013].

To check the effect of the local circulations on the UHI development, the UHI intensities in the southern and northern Singapore are compared in both asymmetric (SURB and NURBS, Figure 5a) and symmetric (HURBS-south and HURBS-north, Figure 5c) urbanization experiments. It appears that during early morning when the land breeze comes from the Malay Peninsula, urbanization in the north leads to a smaller UHI intensity than urbanization in the south; from late morning to early evening, the sea breeze blows northward from the Singapore Strait, and urbanization in the north causes a larger UHI intensity than urbanization in the south. A paired, unequaled *t* test confirms that the above observations are statistically significant, with p value < 0.01 for the comparison between SURB and NURBS experiments and p value < 0.05 for that between HURBS-south and HURBS-north experiments. A further look at the energy balance change of each experiment relative to FOREST (Figures 5b and 5d) shows that UHI intensity difference in the early morning is caused by the difference in T_s across different experiments (see Figure 4) since Q_H does not show much difference at that time. In contrast, during daytime, around noon in particular, the UHI intensity difference is caused by the difference of Q_H. At the same time, the southern part shows higher Q_E than the northern part, which is of similar magnitude as the difference of Q_H. This is likely due to the sea breeze at that time, bringing moisture to the southern part, while blowing heat away to the northern part.

The effect of local circulations on the UHI development can also be explained in another way. Usually, the higher UHI intensity occurs in the downwind part of the urban area, as observed in *Zhang et al.* [2011]. The reason is that as the air parcels travel, the increase in advected heat results in a higher surface air temperature in the downwind areas. *X.-X. Li et al.* [2013] show that the vertical wind below 1500 m is about 0.1–0.2 m s^{-1}, and thus, the vertical mixing is limited in this process and can be ignored.

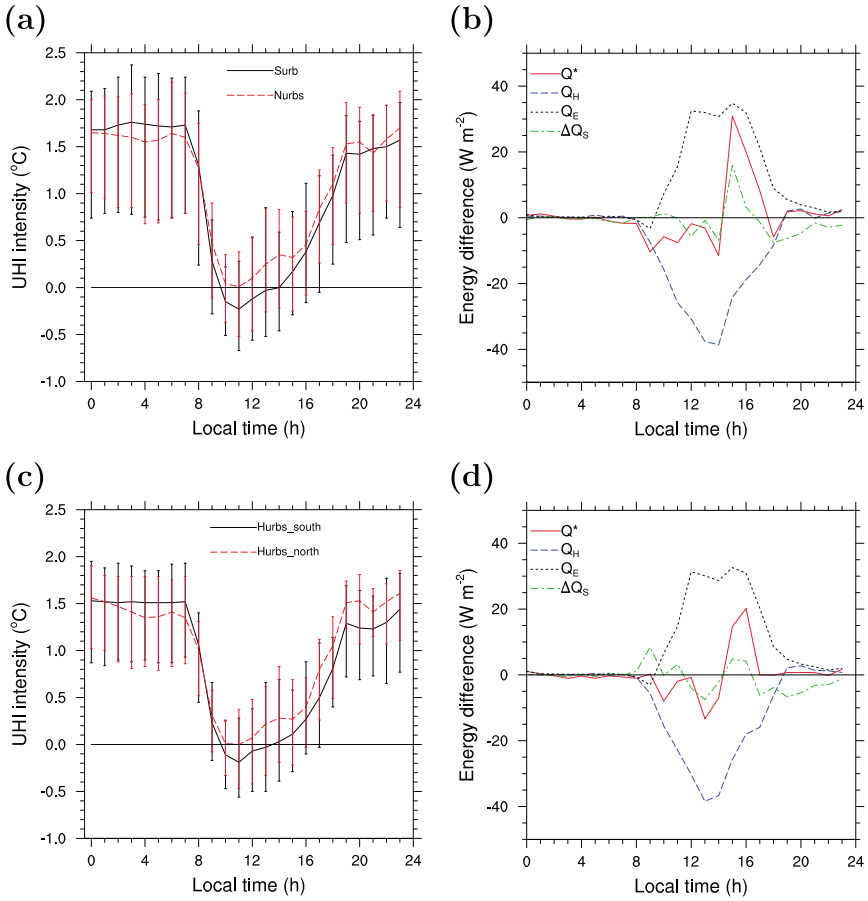

Figure 5. Comparison between the southern and northern parts in both (a) UHI intensity in asymmetric (SURB and NURBS); (b) difference of energy change relative to FOREST in asymmetric (SURB and NURBS); (c) UHI intensity in symmetric (HURBS); and (d) difference of energy change relative to FOREST in symmetric (HURBS) urbanization patterns. The vertical bars indicate the maximum and minimum UHI intensities.

3.1.4. Effect of Anthropogenic Heat

The AH associated with urbanization has been shown to have a great impact on the urban thermal conditions and boundary layer structure [e.g., *X.-X. Li et al.*, 2013; *Bohnenstengel et al.*, 2014]. The results shown in the previous sections are for the experiments with the same amount of AH, while in this section the results from the experiments with different AH will be investigated.

Figures 6a and 6c show the comparison of UHI intensities between the experiments with the same urbanization pattern, different peak values of AH but roughly the same domain-averaged sensible heat flux at the surface. The UHI intensity from the NURB experiment is significantly higher than that from NURBS (p value < 0.01), while the UHI intensity from the HURB-south is slightly higher than that from HURBS-south (p value < 0.01 except for 14:00 LT). Evidently, this discrepancy is caused by the larger difference in AH values between NURB and NURBS experiments than that between HURB and HURBS (see Table 1), which is also revealed in the difference of Q_H change relative to the FOREST experiment (Figures 6b and 6d). The diurnal change of Q_H between NURB/NURBS and between HURB-south/HURBS-south is highly correlated with the AH diurnal profile, showing clearly the dominance of AH in both the Q_H and T_s (Figure 7). Another interesting point to note from Figures 6a and 6c is that the difference caused by AH is more obvious during nighttime than during daytime, a natural result of the indirect AH effect on T_2 through equation (2).

3.2. Rainfall

3.2.1. Model Evaluation

Before we further examine the effect of urbanization patterns on the rainfall, a performance evaluation of the current WRF/UCM coupled system in predicting rainfall is first carried out. The rainfall data from a gauge network (Figure 8a) maintained by Meteorological Service Singapore (MSS) will be used for this purpose.

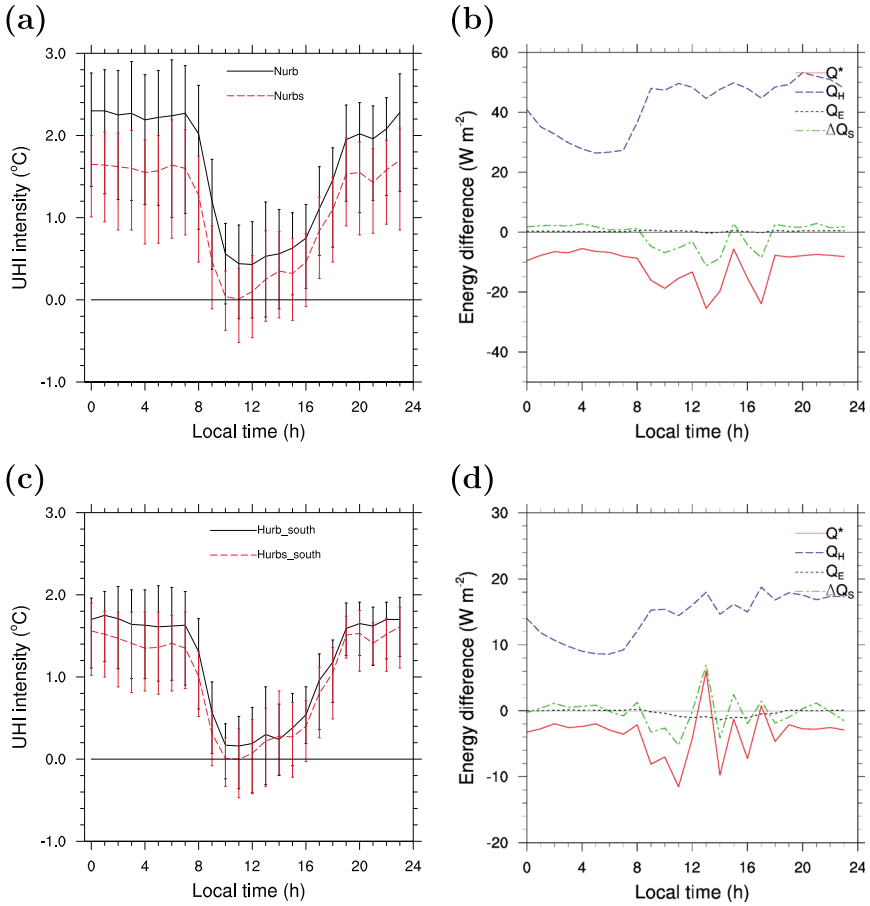

Figure 6. Comparison between the experiments with same urbanization pattern but different amount of AH. (a) UHI intensity in NURB and NURBS; (b) difference of energy change in NURB and NURBS relative to FOREST; (c) UHI intensity in HURB_South and HURBS_South; and (d) difference of energy change in HURB_south and HURBS_south relative to FOREST. The vertical bars indicate the maximum and minimum UHI intensities.

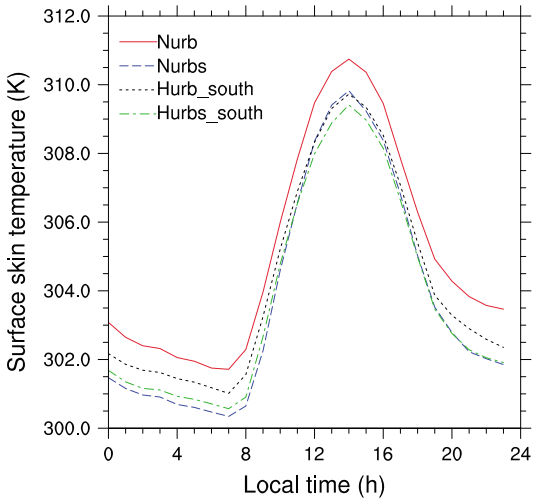

Figure 7. The averaged surface skin temperatures T_s in NURB, NURBS, and HURB_south and HURBS_south, which are calculated over all the urban grid cells in the respective experiments.

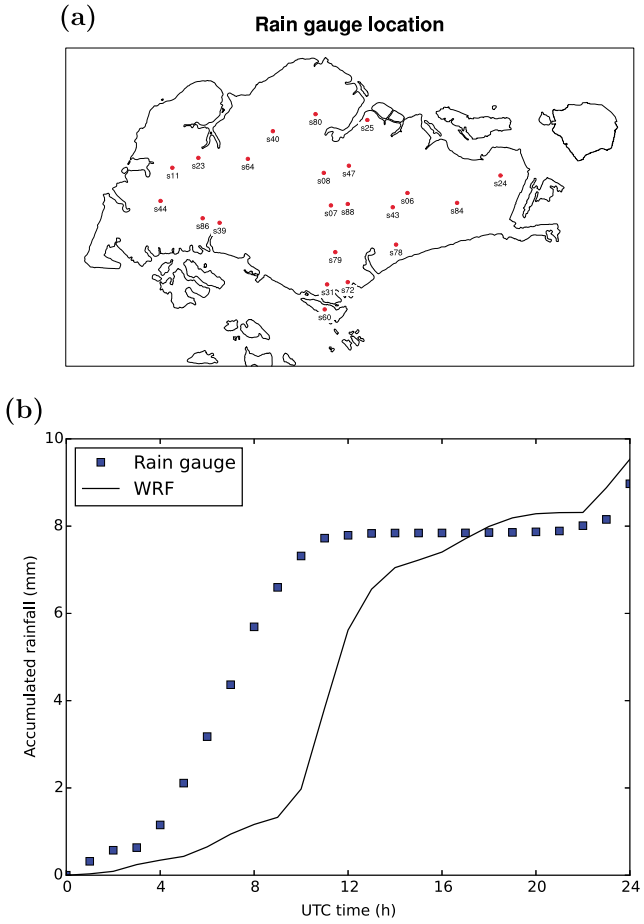

Figure 8. (a) The distribution of the 22 rain gauges around Singapore maintained by Meteorological Service Singapore (MSS). (b) The comparison of the accumulative rainfall amount averaged over the 22 rain gauge locations and the 28 ensemble member cases in the observations (dots) and model runs (line).

This model evaluation will hopefully provide some confidence in the model performance and, on the other hand, help to understand the possible uncertainties when we interpret the results in the upcoming sections. It should be noted that due to the case selection criteria (intermonsoon season), the accumulated rainfall amount is low so that the effect of rainfall on UHI is minimum.

Figure 8b shows the comparison of the simulated (from CONTROL experiment) and observed accumulated rainfall averaged over all the ensemble members and rain gauges. While the 24 h accumulated rainfall amount agrees very well between the simulation results and rain gauge measurement, the simulated onset of the rainfall is about 5 h later than the observed time. A further comparison of the observed and simulated rainfall for each station (not shown here) reveals that, generally, the predicted timing of rainfall for the stations along the coast is worse than that for the inland stations, while the predicted accumulated rainfall amount is better for the stations along the coast. This may be caused by the underprediction of the sea breeze speed by the WRF model. In other reported studies with the WRF model in temperate regions, usually, the simulated onset of rainfall is about 4 h earlier than the observed time due to the faster wind speed predicted by the model [*Y. Zhang et al.*, 2009; *Miao et al.*, 2011; *D. Li et al.*, 2013]. It is expected that the delayed onset will not affect the conclusions in the upcoming sections since none of the effects examined will be based on the temporal accuracy.

Since most of the rainfall occurs in the afternoon when the wind (sea breeze) blows northward or northeastward over Singapore island, it is natural to define a "downwind" region as shown in Figure 9 to investigate the rainfall change in different urbanization experiments.

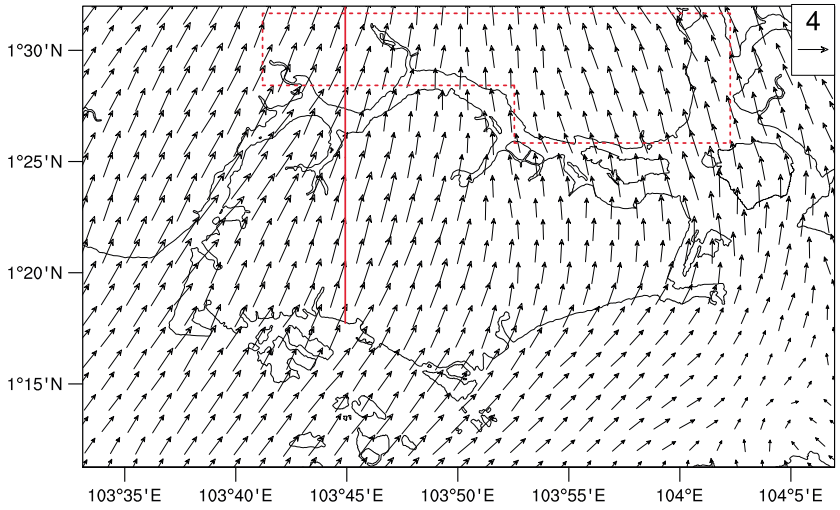

Figure 9. The 10 m wind vector (unit: m s^{-1}) averaged over 28 members at 17:00 LT from the CONTROL case and the definition of the downwind region (the red dashed line) for the comparison of urban and downwind rainfall amount in the NURB and NURBS experiments. The solid red line indicates the location of the cross section in Figure 11.

3.2.2. Effect of Urbanization and Associated Anthropogenic Heat

In the same urbanization pattern (NURB and NURBS experiments), if the AH associated with the urban area is not high enough (NURBS), the rainfall amount in the urban area is lower than that in the corresponding area of the FOREST experiment (FOREST-north), and the rainfall amount in the downwind region (Southern Malaysia) is higher. However, if the urban AH is high enough (NURB), the opposite is true (Figure 10).

To explain the above observation, some important notes must be made. First, the evergreen broadleaf forest land use type used in this study has a lower albedo (0.12) than that of the urban area (0.20) since the incident radiation can penetrate deeply into the forest canopy and get trapped there [*Dobos*, 2006]. As a result, the northern part of the FOREST experiment (forest) may have a higher T_s and sensible heat flux than the northern part (urban) of NURB and NURBS if the associated AH is not taken into account. Second, the associated AH becomes the key to determining the difference in surface buoyancy between the NURB/NURBS and FOREST experiments. Figure 11 shows the vertical structure along the line cutting across Singapore and Southern Malaysia (see Figure 9) at 17:00 LT. With a higher AH, the NURB experiment shows a stronger surface buoyancy in northern Singapore than the FOREST experiment (Figure 11a), whereas the NURBS experiment

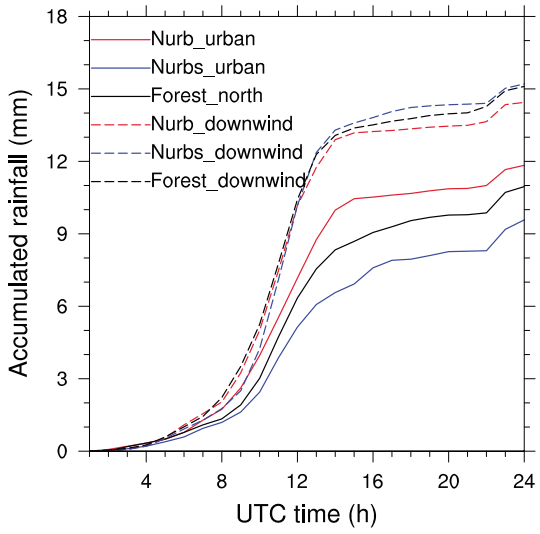

Figure 10. Comparison of the accumulated rainfall in the urban and downwind regions of the NURB, NURBS, and FOREST experiments.

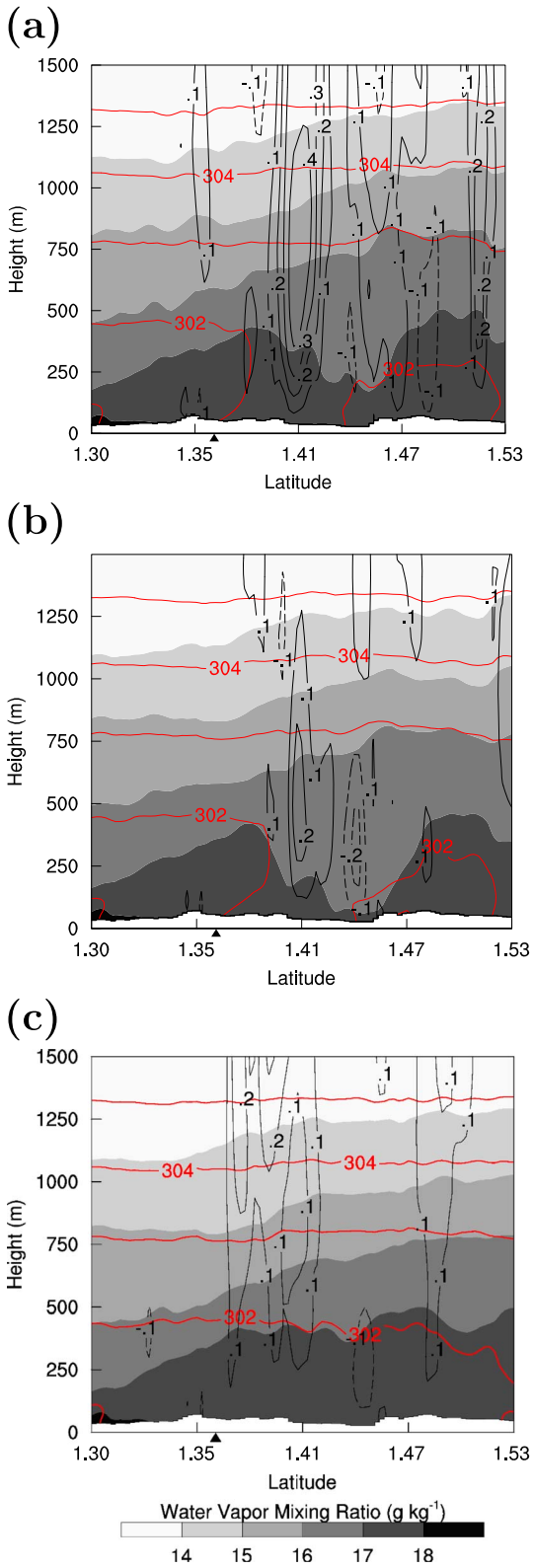

Figure 11. Vertical cross section (along the red line shown in Figure 9) showing potential temperature (K, red solid lines), water vapor mixing ratio (g kg^{-1}, gray scale shades) and vertical velocity at 0.1 m s^{-1} intervals (black lines, with solid lines for upward motion and dashed lines for downward motion) in (a) NURB; (b) NURBS; and (c) FOREST experiments at 17:00 LT. The triangle shows the demarcation of southern and northern Singapore.

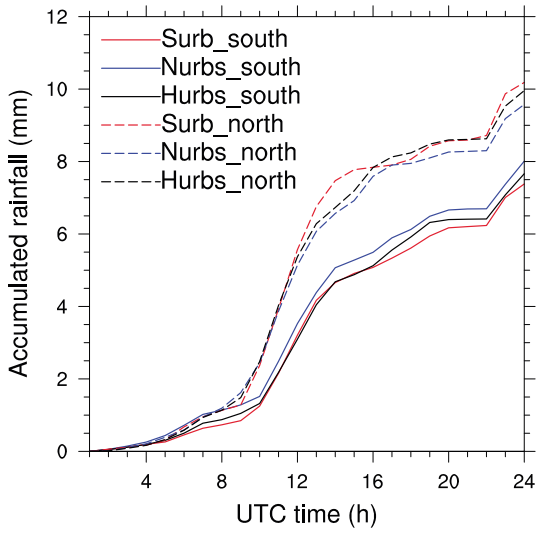

Figure 12. Comparison of the accumulated rainfall in the southern and northern parts of the SURB, NURBS, and HURBS experiments.

has a weaker buoyancy (Figure 11b). Subsequently, the NURB experiment, with stronger buoyancy and thus stronger convection (0.4 m s^{-1}), sees more rainfall amount in the northern part and leaves less moist air to the downwind part. It also can be seen from Figure 11 that the increasing AH in the northern Singapore can also strengthen the convection in the downwind region, but the effect on the rainfall amount in the downwind region is small.

In summary, urbanization will affect the rainfall amount in two ways: (1) enhance rainfall by providing greater buoyancy of surface air encouraging local convection and (2) reduce rainfall by less local moisture source due to the elimination of greenery. Eventually, the overall impact of urbanization will depend on the relative influence of these two effects. The higher AH means higher surface buoyancy (see Figures 11a and 11b) and leads to the dominance of buoyancy effect.

3.2.3. Effect of Urbanization Pattern

In the different urbanization patterns (SURB, NURBS, and HURBS experiments) with the same AH, the comparison in Figure 12 shows that for the same experiment, northern Singapore always experiences more rainfall than southern Singapore because northern Singapore is nearer to the center of sea breeze convergence located in southern Peninsular Malaysia. This observation is statistically significant for SURB and HURBS (p value < 0.05), but not for NURBS (p value ≈ 0.07). Since the different urbanization patterns do not change much the sea breeze development when most of the rainfall occurs, it seems to suggest that the sea breeze has stronger influence on local rainfall than urbanization patterns. Given the fact that the sea breeze speed is about 4 m s^{-1} at the 10 m level and the relatively small extent of Singapore island (especially in the north-south direction, about 20 km), the sea breeze can sweep over Singapore in about 1.5 h. Therefore, the stronger influence of the sea breeze may not be a surprise.

Comparing the SURB and NURBS experiments where AH is equally weak (Figure 12), moving the urbanization from the south to the north slightly enhances the southern rainfall (see Surb-south and Nurbs-south) because of the local enhancement of latent heat flux. Downwind of the sea breeze in northern Singapore, rainfall is correspondingly reduced (see Surb-north and Nurbs-north) due to the decrease in water vapor supply after enhanced rain-out in the south. This partly explains the statistical insignificance of the comparison between the rainfall amount in northern and southern Singapore in the NURBS experiment, as noted above.

It is interesting to observe in Figure 12 that both in the southern and northern parts, the rainfall amounts from the HURBS experiment are generally in-between those from SURB and NURBS experiments. This is the result of the symmetric distribution of urban and forest areas in the HURBS experiment. The homogeneous setting of land use types seems to help distribute the rainfall more evenly within the southern and northern parts. This is different from the situation for UHI intensity (see section 3.1.2); in the asymmetric urbanization experiments

(SURB and NURBS), the UHI intensity is always higher than in the symmetric urbanization experiment (HURBS). This reveals that the impact of symmetric urbanization on a physical variable is highly dependent on what physical mechanisms affect it.

4. Conclusion

As an extreme case of land cover/land use change, urbanization has strong impacts on local climate, especially in such tropical coastal cities as Singapore. This paper examines the effect of urbanization and urbanization patterns on the urban thermal environment and rainfall using the coupled WRF-urban canopy model in ensemble experiments. The urbanization pattern changes are represented by several idealized scenarios: the asymmetric urbanization SURB (the southern part of Singapore is urban while the northern part is forested), and NURB (the northern part of Singapore is urban while the southern part is forested), and the symmetric urbanization HURB (the whole Singapore is covered by alternating urban and forest land use types. Additional scenarios, NURBS and HURBS, which use the same urbanization pattern as in NURB and HURB but with the same anthropogenic heat (AH) profile as in SURB, are also considered to evaluate the effect of AH.

The results from the 28 members of the ensemble for different urbanization scenarios show that both urbanization patterns and AH have some impact on the urban heat island (UHI) intensity, although the impact of urbanization patterns is rather weak. In the asymmetric urbanization patterns (SURB and NURBS), the magnitude of UHI intensity is mildly higher than that in the symmetric urbanization pattern (HURBS) due to the contiguous distribution of urban areas in the former. On the other hand, the changes induced by altering anthropogenic heat are much more significant. Higher AH will induce higher UHI intensity, and the effect of AH is more prominent during the nighttime than daytime, which is consistent with the findings from *X.-X. Li et al.* [2013]. The climate of urban areas and downwind of urban areas seems to be sensitive to AH intensity, which can come about more readily (e.g., by increasing the use of air conditioners at night) than major changes in urbanization patterns. The local circulations (sea/land breezes) will cool the upwind area, and air parcels travel downwind with the heat flux accumulated from upwind areas, making the downwind area hotter.

The rainfall in tropical coastal cities can often be driven by local sea breezes. Sea breezes bring moist air into Singapore during late morning and afternoon. Our study suggests that sea breezes have stronger influence on rainfall than the urbanization pattern since the downwind part (northern Singapore) always has more rainfall than the upwind part (southern Singapore) even in experiments where the urbanization pattern is entirely reversed. The urbanization and the associated AH can increase rainfall through increasing buoyancy by AH or decrease rainfall through reducing evaporation by converting greenery to impervious surfaces. The ultimate effect is determined by the relative strength of these two influences.

While it is natural to presume that the results of the symmetric urbanization experiment always lie in between those of the asymmetric urbanization experiments, the UHI intensities in both asymmetric urbanization experiments (SURB and NURBS) are higher than that from HURBS. On the other hand, the rainfall amount from the HURBS experiment does indeed lie between those from the SURB and NURBS experiments most of the time. This different behavior indicates that the effect of having uniform urbanization patterns is not always the same and is, in fact, dependent on the dynamics governing the examined physical variable.

While evidence points strongly to a role for aerosols in urban precipitation modification, the details of that role still remain highly uncertain [*Shepherd*, 2005]. Furthermore, the WRF model itself cannot predict the aerosol distribution without coupling with other photochemical models such as WRF-Chem. In addition, our focus is the effect of changing urbanization patterns, which is supposed to modify little, if any, the aerosol effect between different urbanization patterns, and hence, the aerosol effect will not affect the results and conclusions that are based on the difference caused by urbanization pattern change. Therefore, we have left out the aerosol effect from urbanization in this study regardless of its importance.

Acknowledgments
This project was funded by Singapore National Research Foundation (NRF) through the Singapore-MIT Alliance for Research and Technology (SMART) Center for Environmental Sensing and Modeling (CENSAM). The land use/land cover data for Singapore were purchased from Center of Remote Imaging, Sensing and Processing (CRISP), National University of Singapore. The rainfall gauge data were obtained through collaboration with Meteorological Service Singapore (MSS). The input and output data (excluding the purchased data) used in the studies are available from the corresponding author upon request (lixx@smart.mit.edu), provided that they are used solely for academic research purpose.

References

Bohnenstengel, S. I., S. Evans, P. A. Clark, and S. Belcher (2011), Simulations of the London urban heat island, *Q. J. R. Meteorol. Soc.*, *137*, 1625–1640.

Bohnenstengel, S. I., I. Hamilton, M. Davies, and S. E. Belcher (2014), Impact of anthropogenic heat emissions on London's temperatures, *Q. J. R. Meteorol. Soc.*, *140*(679), 687–698.

Bornstein, R., and Q. Lin (2000), Urban heat islands and summertime convective thunderstorms in Atlanta: Three case studies, *Atmos. Environ.*, *34*(3), 507–516.

Boutle, I. A., J. E. J. Eyre, and A. P. Lock (2014), Seamless stratocumulus simulation across the turbulent gray zone, *Mon. Weather Rev.*, *142*(4), 1655–1668.
Burian, S. J., J. M. Shepherd, and P. Hooshialsadat (2004), Urbanization impacts on Houston rainstorms, in *Innovative Modeling of Urban Water Systems*, edited by W. James, pp. 1–22, CHI, Geulph, Canada.
Changnon, S. A. (1968), The LaPorte weather anomaly—Fact or fiction?, *Bull. Am. Meteorol. Soc.*, *48*, 4–11.
Chen, F., et al. (2011), The integrated WRF/urban modelling system: Development, evaluation, and applications to urban environmental problems, *Int. J. Climatol.*, *31*(2), 273–288.
Chia, L. S., and S. F. Foong (1991), Climate and weather, in *The Biophysical Environment of Singapore*, edited by L. S. Chia, A. Rahman, and D. B. H. Tay, pp. 13–49, Singapore Univ. Press and the Geogr. Teachers' Associ. of Singapore, Singapore.
Chow, W. T. L., and M. Roth (2006), Temporal dynamics of the urban heat island of Singapore, *Int. J. Climatol.*, *26*(15), 2243–2260.
Dobos, E. (2006), Albedo, in *Encyclopedia of Soil Science*, edited by R. Lal, pp. 64–66, Taylor and Francis, Boca Raton, Fla., doi:10.1081/E-ESS-120014334.
Efstathiou, G. A., and R. J. Beare (2015), Quantifying and improving sub-grid diffusion in the boundary-layer grey zone, *Q. J. R. Meteorol. Soc.*, *141*(693), 3006–3017.
Essenwanger, O. M. (2001), Classification of climates, in *World Survey of Climatology 1C: General Climatology*, pp. 1–102, Elsevier, Amsterdam.
Georgescu, M., M. Moustaoui, A. Mahalov, and J. Dudhia (2013), Summer-time climate impacts of projected megapolitan expansion in Arizona, *Nat. Clim. Change*, *3*(1), 37–41.
Georgescu, M., P. E. Morefield, B. G. Bierwagen, and C. P. Weaver (2014), Urban adaptation can roll back warming of emerging megapolitan regions, *Proc. Natl. Acad. Sci. U.S.A.*, *111*(8), 2909–2914.
Georgescu, M., W. T. L. Chow, Z. H. Wang, A. Brazel, B. Trapido-Lurie, M. Roth, and V. Benson-Lira (2015), Prioritizing urban sustainability solutions: Coordinated approaches must incorporate scale-dependent built environment induced effects, *Environ. Res. Lett.*, *10*(6), 061001.
Green, B. W., and F. Zhang (2015), Numerical simulations of hurricane Katrina (2005) in the turbulent gray zone, *J. Adv. Model. Earth Syst.*, *7*(1), 142–161.
Grimmond, C. S. B., and T. R. Oke (1999), Heat storage in urban areas: Observations and evaluation of a simple model, *J. Appl. Meteorol. Climatol.*, *38*, 922–940.
Heisler, G. M., and A. J. Brazel (2010), The urban physical environment: Temperature and urban heat islands, in *Urban Ecosystem Ecology, Agron. Monogr.*, vol. 55, edited by J. Aitkenhead-Peterson and A. Volder, pp. 29–56, ASA, CSSA, and SSSA, Madison, Wisc.
Honnert, R., V. Masson, and F. Couvreux (2011), A diagnostic for evaluating the representation of turbulence in atmospheric models at the kilometric scale, *J. Atmos. Sci.*, *68*(12), 3112–3131.
Huff, F. A., and S. A. Changnon (1972), Climatological assessment of urban effects on precipitation at St. Louis, *J. Appl. Meteorol.*, *11*, 823–842.
Hunt, J. C., Y. V. Timoshkina, S. I. Bohnenstengel, and S. Belcher (2013), Implications of climate change for expanding cities worldwide, *Proc. ICE Urban Design Plan*, *166*(4), 241–254.
Ichinose, T., K. Shimodozono, and K. Hanaki (1999), Impact of anthropogenic heat on urban climate in Tokyo, *Atmos. Environ.*, *33*, 3897–3909.
Ito, J., H. Niino, M. Nakanishi, and C.-H. Moeng (2015), An extension of the Mellor–Yamada model to the terra incognita zone for dry convective mixed layers in the free convection regime, *Boundary Layer Meteorol.*, *157*(1), 23–43.
Joseph, B., B. C. Bhatt, T. Y. Koh, and S. Chen (2008), Sea breeze simulation over the Malay Peninsula in an intermonsoon period, *J. Geophys. Res.*, *113*, D20122, doi:10.1029/2008JD010319.
Kusaka, H., and F. Kimura (2004), Coupling a single-layer urban canopy model with a simple atmospheric model: Impact on urban heat island simulation for an idealized case, *J. Meteorol. Soc. Jpn.*, *82*, 67–80.
Landsberg, H. E. (1970), Man-made climate changes, *Science*, *170*, 1265–1274.
Landsberg, H. E. (1981), *The Urban Climate, Int. Geophys. Ser.*, vol. 28, Academic Press, New York.
Li, D., and E. Bou-Zeid (2014), Quality and sensitivity of high-resolution numerical simulation of urban heat islands, *Environ. Res. Lett.*, *9*, 055001.
Li, D., E. Bou-Zeid, M. L. Baeck, S. Jessup, and J. A. Smith (2013), Modeling land surface processes and heavy rainfall in urban environments: Sensitivity to urban surface representations, *J. Hydrometeorol.*, *14*(4), 1098–1118.
Li, X.-X., T.-Y. Koh, D. Entekhabi, M. Roth, J. Panda, and L. K. Norford (2013), A multi-resolution ensemble study of a tropical urban environment and its interactions with the background regional atmosphere, *J. Geophys. Res. Atmos.*, *118*, 9804–9818, doi:10.1002/jgrd.50795.
Lim, J. T., and A. A. Samah (2004), *Weather and climate of Malaysia*, Univ. of Malaya Press, p. 170, Kuala Lumpur, Malaysia.
Lin, C.-Y., F. Chen, J. Huang, Y. A. Liou, W. C. Chen, W. N. Chen, and S. C. Liu (2008), Urban heat island effect and its impact on boundary layer development and land-sea circulation over northern Taiwan, *Atmos. Environ.*, *42*, 5639–5649.
Lowry, W. (1998), Urban effects on precipitation amount, *Prog. Phys. Geogr.*, *22*, 477–520.
Miao, S., F. Chen, M. LeMone, M. Tewari, Q. Li, and Y. Wang (2009), An observational and modeling study of characteristics of urban heat island and boundary layer structures in Beijing, *J. Appl. Meteorol. Climatol.*, *48*(3), 484–501.
Miao, S., F. Chen, Q. Li, and S. Fan (2011), Impacts of urban processes and urbanization on summer precipitation: A case study of heavy rainfall in Beijing on 1 August 2006, *J. Appl. Meteorol. Climatol.*, *50*(4), 806–825.
Oke, T. R. (1976), The distinction between canopy and boundary-layer urban heat islands, *Atmosphere*, *14*(4), 268–277.
Quah, A. K., and M. Roth (2012), Diurnal and weekly variation of anthropogenic heat emissions in a tropical city, Singapore, *Atmos. Environ.*, *46*, 92–103.
Rosenfeld, D., U. Lohmann, G. B. Raga, C. D. O'Dowd, M. Kulmala, S. Fuzzi, A. Reissell, and M. O. Andreae (2008), Flood or drought: How do aerosols affect precipitation?, *Science*, *321*(5894), 1309–1313, doi:10.1126/science.1160606.
Salamanca, F., A. Martilli, and C. Yagüe (2012), A numerical study of the urban heat island over madrid during the DESIREX (2008) campaign with WRF and an evaluation of simple mitigation strategies, *Int. J. Climatol.*, *32*(15), 2372–2386, doi:10.1002/joc.3398.
Shepherd, J. M. (2005), A review of current investigations of urban-induced rainfall and recommendations for the future, *Earth Interact*, *9*, 1–27.
Shepherd, M., T. Mote, J. Dowd, M. Roden, P. Knox, S. C. McCutcheon, and S. E. Nelson (2011), An overview of synoptic and mesoscale factors contributing to the disastrous Atlanta flood of 2009, *Bull. Am. Meteorol. Soc.*, *92*(7), 861–870.
Shin, H. H., and J. Dudhia (2016), Evaluation of PBL parameterizations in WRF at subkilometer grid spacings: Turbulence statistics in the dry convective boundary layer, *Mon. Weather Rev.*, *144*(3), 1161–1177.

Shin, H. H., and S.-Y. Hong (2015), Representation of the subgrid-scale turbulent transport in convective boundary layers at gray-zone resolutions, *Mon. Weather Rev.*, *143*(1), 250–271.

Skamarock, W. C., J. B. Klemp, J. Dudhia, D. O. Gill, D. M. Barker, M. G. Duda, X.-Y. Huang, W. Wang, and J. G. Powers (2008), A description of the Advanced Research WRF version 3, *Tech. Note*, p. 113, NCAR, Boulder, Colo.

Turner, B. L., A. C. Janetos, P. H. Verbug, and A. T. Murray (2013), Land system architecture: Using land systems to adapt and mitigate global environmental change, *Global Environ. Change*, *23*(2), 395–397.

Voogt, J. A. (2002), Urban heat island, in *Causes and Consequences of Global Environmental Change*, vol. 3, edited by I. Douglas, pp. 660–666, John Wiley, Chichester, U. K.

Wyngaard, J. C. (2004), Toward numerical modeling in the "terra incognita", *J. Atmos. Sci.*, *61*(7), 1816–1826.

Zhang, C.-L., F. Chen, S. Miao, Q. Li, X. Xia, and C. Xuan (2009), Impacts of urban expansion and future green planting on summer precipitation in the Beijing metropolitan area, *J. Geophys. Res.*, *114*, D02116, doi:10.1029/2009JD010328.

Zhang, D.-L., Y.-X. Shou, and R. R. Dickerson (2009), Upstream urbanization exacerbates urban heat island effects, *Geophys. Res. Lett.*, *36*, L24401, doi:10.1029/2009GL041082.

Zhang, D.-L., Y.-X. Shou, R. R. Dickerson, and F. Chen (2011), Impact of upstream urbanization on the urban heat island effects along the Washington-Baltimore corridor, *J. Appl. Meteorol. Climatol.*, *50*(10), 2012–2029.

Zhang, Y., J. A. Smith, A. A. Ntelekos, M. L. Baeck, W. F. Krajewski, and F. Moshary (2009), Structure and evolution of precipitation along a cold front in the northeastern United States, *J. Hydrometeorol.*, *10*, 1243–1256.

Zhao, L., X. Lee, R. B. Smith, and K. Oleson (2014), Strong contributions of local background climate to urban heat islands, *Nature*, *511*(7508), 216–219.

Zhou, B., J. S. Simon, and F. K. Chow (2014), The convective boundary layer in the terra incognita, *J. Atmos. Sci.*, *71*(7), 2545–2563.

Zhou, D., S. Zhao, L. Zhang, G. Sun, and Y. Liu (2015), The footprint of urban heat island effect in China, *Sci. Rep.*, *5*, 11160, doi:10.1038/srep11160.

Zhou, L., R. E. Dickinson, Y. Tian, J. Fang, Q. Li, R. K. Kaufmann, C. J. Tucker, and R. B. Myneni (2004), Evidence for a significant urbanization effect on climate in China, *Proc. Natl. Acad. Sci. U.S.A.*, *101*, 9540–9544.

Zhou, Y., S. J. Smith, K. Zhao, M. Imhoff, A. Thomson, B. Bond-Lamberty, G. R. Asrar, X. Zhang, C. He, and C. D. Elvidge (2015), A global map of urban extent from nightlights, *Environ. Res. Lett.*, *10*(5), 054011.